RSC Advances

ROYAL SOCIETY OF CHEMISTRY

www.rsc.org/advances

RSC Advances

RSCPublishing

ARTICLE

Phenol adsorption from aqueous solutions by Functionalized Multiwalled Carbon Nanotubes with Pyrazoline Derivative in the presence of ultrasound

Cite this: DOI: 10.1039/xoxxoooooox

Received ooth January 2012,
Accepted ooth January 2012

DOI: 10.1039/xoxxoooooox

www.rsc.org/

H. Tahermansouri, Z. Dehghan, F. Kiani

Carboxylated Multi-wall carbon nanotubes (MWCNTs-COOH) were functionalized with pyrazoline derivative (MWCNT-Py) and used for the removal of phenol from aqueous solutions under ultrasound. The resulting materials were characterized by different techniques, such as Fourier transform infrared spectroscopy, thermogravimetric analysis, and transmission electron microscope. In batch tests, the influences of solution pH, contact time (ultrasonic time), concentration of the phenol and amount of adsorbents on the sorption of phenol onto MWCNT-COOH and MWCNT-Py were investigated. The kinetic data were fitted with pseudo-first order, pseudo-second-order, Elovich and intra-particle diffusion models. Kinetic studies showed that the sorption process with MWCNT-COOH and MWCNT-Py was well described by pseudo-second-order and pseudo-first-order kinetics, respectively. In addition, the adsorption isotherms of phenol from aqueous solutions onto MWCNTs were studied. The six isotherm models: Langmuir (four linear forms), Freundlich, Temkin, Halsey, Harkins-Jura, Flory-Huggins and Fowler-Guggenheim models, were applied to determine the characteristic parameters of adsorption process. The results showed which the interaction among adsorbed molecules is repulsive and there is not association between them. Also, the adsorption isotherm models fitted the data in the order: Langmuir > Freundlich, Halsey > Fowler–Guggenheim > Temkin > Harkins-Jura isotherms.

1. Introduction

The removal of the wastewater pollutions, such as organic and inorganic compounds, has attracted the great attentions toward many researchers. Among the organic compounds, the phenols are very important as they can be used in industries as raw materials or intermediates for production of many drugs, dyes, insecticides, and explosives.[1] Hence, they are permanent contaminants of wastewater when are released into the water.[2] In addition, phenolic compounds are toxic even at low concentrations and can be effect on the health of humans.[3-5]Thus, the elimination of phenol from aqueous solutions is essentiality. It was found in review which adsorption of aromatic compounds and metals by carbon nanotubes (CNTs) are considered as potential treatment technique for removal of various types of contaminants.[6] This application of CNTs can be related to their unique properties such as their large surface areas, diameter, π-π electrostatic interactions, and the shorter equilibrium time than other materials. [7] On the other hands, the application of CNTs as adsorbent are restricted due to less functional groups on the surface. [8] Thus, the surface modification of CNTs with functional groups (such as amino, hydroxyl, amide and carbonyl groups) to increasing the adsorption capacity on adsorbent surfaces is requisiteness.[9] So far, many studies have been carried out to removal of phenolic compounds from aqueous solutions by CNTs, however, only a few reports on modified CNTs have been presented[10-16]. Also, Table 1 compares some functionalized MWCNTs for the removal of different pollutions.

Ultrasound is a very useful tool in intensifying the mass transfer process. Moreover, several reports are presented about the adsorption of organic compounds by various adsorbents under ultrasound condition.[17-20] Therefore, we decided to improve this work. In this current study, MWCNT-COOH firstly were modified by 3,5-diphenyl-4,5-dihydro-1H-pyrazole-1-carboxamide (pyrazoline derivative) to form MWCNT-Py. Then, these MWCNTs were used as the efficient adsorbents for the removal of phenol from aqueous solutions under ultrasound. In this research, the four models of kinetic, pseudo-first order, pseudo-second-order, Elovich, intra-particle diffusion models, and six isotherm models, Langmuir, Freundlich, Temkin, Halsey, Harkins-Jura and Fowler-Guggenheim, were analyzed to get a sufficient knowledge on the mechanism and rate of the adsorption process of phenol on the modified MWCNTs. In fact, the goal of this investigation was to study MWCNT-COOH and MWCNT-Py as adsorbent for removal of phenol from aqueous solutions in the presence of ultrasonic waves.

Table 1. Literature results of the adsorption of different pollutants by modified MWCNTs

CNT	Modification method	Type of pollutions removed	Efficiency of adsorbent	Reference
MWCNTs	Modified with 8-hydroxyquinoline	Cu, Pb, Cd, Zn	The modification significantly enhanced the removal of heavy metals from aqueous solution.	21
MWCNTs	Functionalized with iron oxides and β-cyclodextrin	1-Naphthylamine	adsorption capacity of 200.0 $mg \cdot g^{-1}$	22
MWCNTs	Functionalized with ethylenediamine, cyanuric chloride and sodium 2-mercaptoethanol in sequence	Hg	Hg(II) sorption by MWCNTs-SH is remarkably more than MWCNTs, approximately three folds.	23
MWCNTs	halloysite nanotubes (HNTs) was functionalized by polyethyleneimine (PEI)	Cr	The Cr (VI) uptake capacity of PEI-HNTs was about 64 times higher than that of the original HNTs.	24
MWCNTs	noncovalently wrapped with poly (sodium 4-styrenesulfonate) (PSS)	methylene blue	10 wt% PSS around CNTs doubles the adsorption capacity of methylene blue.	25
MWCNTs	Physical mixing MWCNTs and ferrite ($NiFe_2O_4$)	Aniline	Maximum adsorption of 96.5%	26
MWCNTs	Purified (P-MWCNTs), graphitized (G-MWCNTs), carboxylated (C-MWCNTs), and hydroxylated (H-MWCNTs)	1-Naphthol	Solution chemistry, such as pH and surface oxygen-containing groups on CNTs, plays a significant role in the adsorption.	27
MWCNTs	With 4-Aminophenyl methylphosphonate grafted	4-Chlorophenol	Maximum adsorption of 85.1%	28
MWCNTs	Modified with alumina(Al_2O_3)	Phenol , 4-chlorophenol	CNT-Al_2O_3 showed better adsorption efficiency than CNT which could be assigned to the increase in the surface area.	29
MWCNTs	Copper and silver nanoparticles were immobilized on CNTs, which were then embedded in water insoluble CD polyurethane polymers	para-Nitrophenol	Maximum removal of 55%	30
MWCNTs	Grafted with methyl methacrylate (MMA)	4,4′-DCB	Maximum removal >90%	31
MWCNTs	Oxidized (o-MWCNT) and modified with ethylenediamine (e-MWCNT)	Cd	The maximum capacity was obtained for e-MWCNT, 25.7 mgg^{-1}, at 45°C	32
MWCNTs	modified with Amidoxime	uranium(VI)	The adsorption capacity was found 145 mg g^{-1}	33
MWCNTs	Grafted with Grafted with 3,5-diphenyl-4,5-dihydro-1H-pyrazole-1-carboxamide	Phenol	Present work	

2. Experimental

2.1. Materials and methods

All reagents and solvents (thionyl chloride, tetrahydrofuran(THF), toluene, thiosemicarbazide, benzaldehyde, acetophenone , ethanol, phenol) from Merck Chemical Inc. and MWCNTs (%95 purity, OD: 10-20 nm, Length: 0.5-2 µm, Neutrino Co., Ltd) were purchased and used as received). Pyrazoline derivative is prepared from the reaction of chalcone with thiosemicarbazide.[34]MWCNT-Py was characterized using a Thermo Nicolet Nexus 870 Fourier transform infrared spectroscopy (FT-IR), a Philips CM120 transmission electron microscope (TEM) and a Netzsch TG 209 F1 Iris thermogravimetric analyzer (TGA) under nitrogen gas atmosphere (10°C/min). Analytical reagent-grade chemicals were used as well as deionized water from a Milli-Q system (Millipore). The concentration of phenol was performed by Unico UV-2100 Model variable-wavelength UV-vis spectrophotometric at 269 nm. The ultrasonic irradiation was carried out with Elmasonic S 60 H with constant frequency 37 kHz.

2.2. Preparation of MWCNT-Py

MWCNT-COOH (250 mg) was suspended in 40 mL of $SOCl_2$ and 1 mL of DMF. Then, the mixture was stirred at 70°C for 48 h under reflux. Subsequently, the residual $SOCl_2$ was removed by reduced pressure distillation to yield the acylchloride functionalized MWCNT (MWCNTCOCl). MWCNT-COCl (150 mg) was mixed with 400 mg of pyrazoline derivative in 40 mL of toluene, and the reaction mixture was stirred at 100°C for 96 h. Then, the mixture was cooled to room temperature, filtered and washed thoroughly with ethyl alcohol and THF. Subsequently, the black solid was dried at room temperature for 10 h under vacuum condition.

2.3. Batch Sorption Experiments

To study the effects of pH on the sorption of phenol, 30 mg of a given MWCNT was dispersed into 15 mL solutions containing 50 mg/L of phenol. The initial pH values were adjusted from 3.0 to 10.0 using nitric acid and NaOH and the suspensions were sonicated for 30 min at 25±1 °C. The amounts of sorbed phenol were calculated as the difference between the initial and final concentrations when the equilibrium was reached. The results are based on at least three replicate experiments for each pH value. To estimate the sorption capacity, 30 mg of the appropriate sorbent was mixed with 15 mL of phenol solution (concentration range 10-100 mg/L). After 30 min (25±1°C) of the sonication, the phenol concentration in the aqueous solutions was determined by UV-vis spectroscopy. The removal (%) and sorption capacity q (mg/g) was obtained as follows:

$$\textbf{Removal}\ \% = \frac{C_0 - C_e}{C_0} \times 100\% \qquad q_e = \frac{(C_0 - C_e) \times V}{m}$$

where C_0 and C_e are the initial and final concentrations (mg/L) of phenol in the aqueous solution, respectively, V (L) is the volume of phenol solution, and m (g) is the weight of sorbent. The kinetic data were analyzed using four kinetic models to gain an understanding of the sorption process. The kinetic experiment was carried out under normal atmospheric conditions at 25±1°C. Initially, 30 mg of MWCNTs contacted with 15 mL solution containing 50 mg L^{-1} phenol concentration in glass vials and then it were sonicated for the different times. Adsorbent and solution were separated at predetermined time intervals, filtered using a 0.45 µm membrane filter and analyzed for residual phenol concentrations as described in above.

2.4. Kinetic models

Four kinetic models, namely, pseudo-first-order, pseudo-second-order, Weber-Morris intra-particle diffusion and Elovich models are used to investigate the mechanism of phenol adsorption**.**

2.4.1. Pseudo-first-order model

The pseudo-first-order equation, which is proposed by Lagergren,[35] has been used for reversible reaction with an equilibrium being established between liquid and solid phases. This equation is expressed as follows:

$$\log(q_e - q_t) = \log(q_e) - \frac{k_1}{2.303}\, t$$

where k_1 is the rate constant of adsorption (min^{-1}), q_e is the amount adsorbed (mg/g) at equilibrium and q_t is the amount adsorbed (mg/g) at time t. The plot of $\log(q_e - q_t)$ against t gives a linear relationship from which k_1 and q_e are determined from the slope and intercept of plot, respectively.

2.4.2. Pseudo-second-order model

The pseudo-second-order model may be expressed as given in linear form: [36]

$$\frac{t}{q_t} = \frac{1}{k_2 q_e^2} + \frac{1}{q_e}\, t$$

where k_2 is the pseudo second-order rate constant of adsorption (g/mg min), other terms has already been defined. The values of q_e and k_2 can be estimated from the slope and intercept of the plot of t/q_t versus t.

2.4.3. Elovich model

Elovich's[37,38] equation assumes which the solid surfaces of adsorbent are energetically heterogeneous and there are not desorption and interaction between the adsorbed species at low surface coverage. This model can be expressed to the linear form as follows:

$$q_t = \frac{1}{b}\ln(ab) + \frac{1}{b}\ln(t)$$

The parameter a of the equation is the initial sorption rate (mg/g min), while the parameter b is related to the extent of surface coverage and activation energy for chemisorption (g/mg). If this equation applies, it should lead to a straight line which a and b coefficients can be calculated from the plot of q_t versus ln t.

2.4.4. Intra-particle diffusion model

The intra-particle diffusion model [36,39] is used to identifying the mechanism involved during adsorption process, described by external mass transfer and intra-particle diffusion. This model enables investigation of the possibility of intra-particle

a)

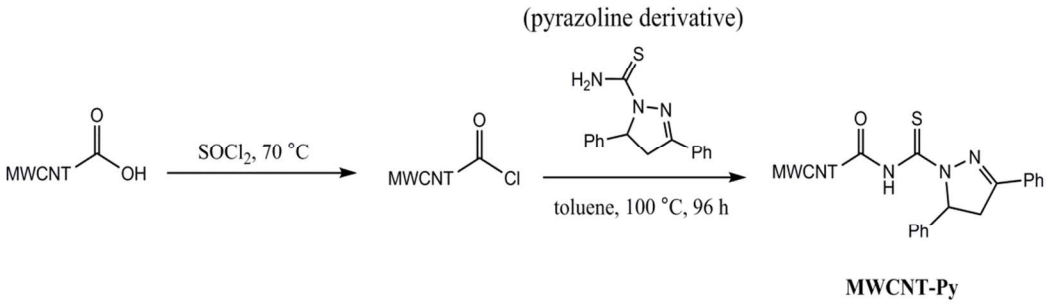

b)

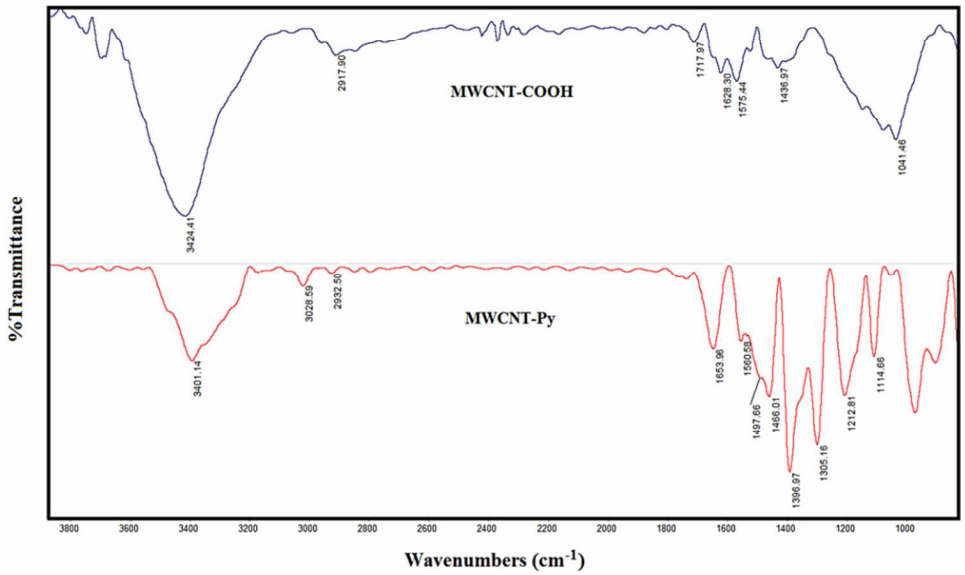

Fig 1. (a) Reaction paths for introduction of 2-aminobenzamide groups on MWCNTs. (b) FT-IR spectra (after baseline correction) of modified MWCNTs.

diffusion by using the following equation:

$$q_t = k_{id} t^{0.5} + C_i$$

where k_{id} (mole $g^{-1}min^{1/2}$) is the rate constant of intra-particle diffusion and C_i is proportional to the boundary layer thickness. If the regression of q_t versus $t^{1/2}$ gives a straight line, then intra-particle diffusion is involved in the adsorption process and if this line passes through the origin, then intraparticle diffusion is the sole rate-limiting step and k_{id} can be calculated from the slope and C_i from the intercept. The validity of the above four models was checked by studying the kinetics under ultrasonic wave.

3. Results and discussion

3.1. Characterization of MWCNT-Py

Figure 1a illustrates the procedure for functionalization of MWCNTs by pryazoline derivative. The product was characterized by FT-IR, TGA, and TEM. Figure 1b presents the FT-IR spectrum of modified MWCNTs. In MWCNT-COOH, the peaks at 1575 and 3424 cm^{-1} is assigned to the C=C and OH stretching modes, respectively. In addition, the appearance of the absorption peaks at 1717(C=O) and 1041(C-O) cm^{-1} clearly shows carboxylic groups on the MWCNTs.[40]

In the spectrum of MWCNT-Py, the new peaks at 1653 and 1114 cm^{-1} can be assigned to the amide group (as compared to 1717 cm^{-1} for MWCNTs-COOH) and C=S mode,[36] respectively which confirmed the formation of MWCNT-Py. In addition, the peaks at around 3200-3500, 3028, 1500-1600, 1300-1500 and 1000-1200 cm^{-1} correspond to N-H stretching mode, C-H aromatic ring, C=C or C=N modes, C-N and C-O stretching modes, respectively. Also, the band at around 2910-2940 which seen in both spectra can be related to the C–H stretch vibration of the sidewalls. Thus, FT-IR spectra confirm that MWCNT-COOH has been successfully modified by pyrazoline derivative.

TEM images of MWCNT-COOH and MWCNT-Py was presented in Figure 2. The average of the outer diameters and inner cavities of MWCNTs were obtained 15-25 nm and 3-7 nm, respectively. In addition, these images show that they are curved and entangled with each other. Also, many agglomerates in the MWCNTs are observed.

Thermal defunctionalization, thermogravimetric analysis (TGA), is the best evidence for the functionalization of MWCNTs which can be provided the useful information concerning the functionalization of MWCNTs. According to Figure 3, since the TGA curve of MWCNT-COOH is almost thermally stable, the weight loss before decomposition of MWCNTs can be used to estimate the quantity of various groups attached to nanotube. As can be seen in Figure 3,

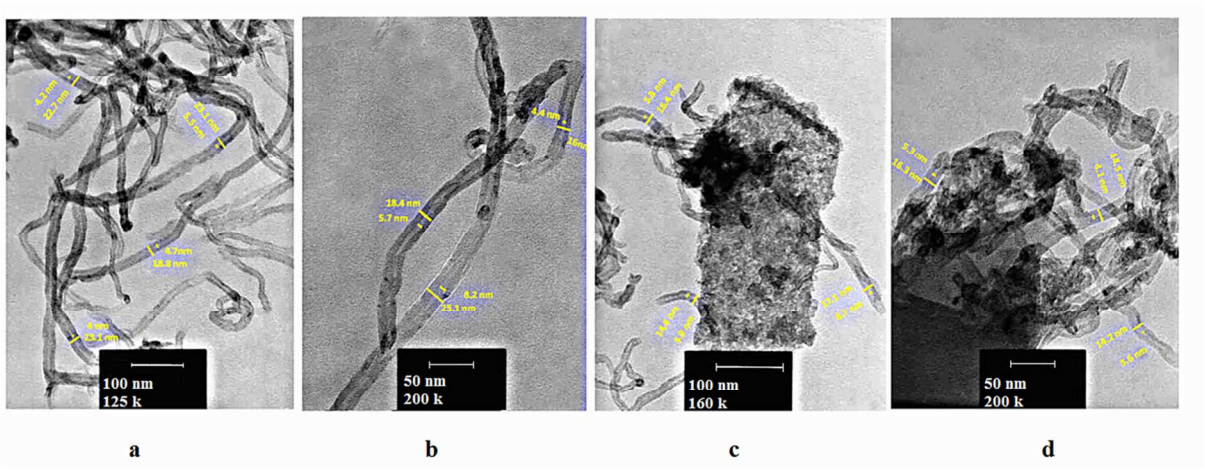

Fig 2. TEM images of the MWCNT-COOH (a,b) and MWCNT-Py (c,d) at different magnifications.

MWCNT-Py sample exhibits one major decomposition at around 160-280 ℃ with a weight loss about 14.33% which can be assigned to decomposition of the attached pyrazoline derivative to MWCNTs. On the basis, the fraction of carbon atoms that are functionalized with pyrazoline derivative groups in 280 ℃ was calculated to be about 0.74 wt. %.

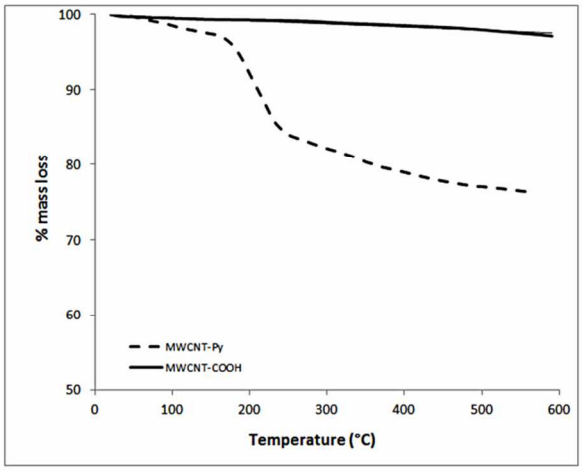

Fig 3. TGA curve of modified MWCNTs in the N_2 (10˚C /min).

3.2. Adsorption studies

3.2.1. Effect of Contact Time

The removal percentage of phenol by MWCNTs as a function of contact time is presented in Figure 4. As it is shown, in the ultrasound method, at up to 15 min for MWCNT-COOH and 20 min for MWCNT-Py of initial contact time, the phenol adsorption rate was relatively rapid and then reached equilibrium at nearly 20 min for MWCNT-COOH and 25 min for MWCNT-Py. In the stirring method, the uptake of phenol from solution was reduced by both MWCNTs. The observed differences can be related to the better mass transfer in the presence of ultrasound and the influence of ultrasound on the carbon nanotubes. According to the Figure 4, the removal of phenol with MWCNT-COOH and MWCNT-Py in 30 min was 30.5% and 99.2%, respectively, under sonication. But, in the same conditions in stirring method the final value of the adsorption percentage of phenol was found to be 17.8 % (MWCNT-COOH) and 63.2% (MWCNT-Py). These values are noticeable for MWCNT-Py which can be related to the presence of lots of accessible sites (external surface sorption) on the MWCNT-Py surface (as compared to MWCNT-COOH) that follows the fast transfer of phenol species to the surface of CNTs at time 5-20 min.

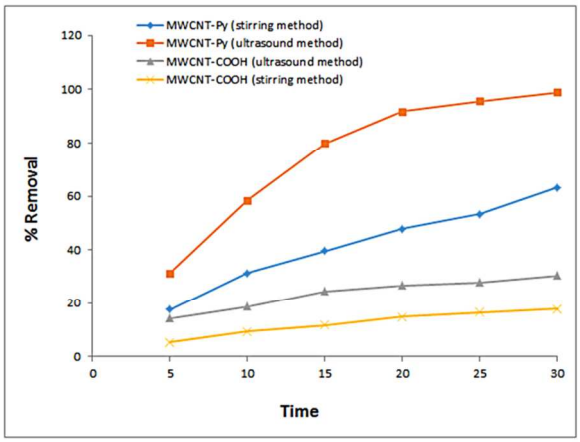

Fig 4. Effect of contact time on the adsorption of phenol from aqueous solution by both MWCNTs (experimental conditions: pH=7; MWCNTs mass, 30mg/15 mL; phenol concentration, 50 mg/L).

3.2.2. Effect of CNT Dosage

Dosage studies were carried out to determine the adsorption percentage of phenol from aqueous solutions at a phenol concentration of 50 mg/L. According to Figure 5a, the experimental results revealed that the adsorption percentage of phenol increase with increasing MWCNT dosage and the ultrasonic time was kept at 30 min. For example, the removal of phenol significantly enhanced from 28% to 56.4% for MWCNT-COOH and 49.9 to 94 % for MWCNT-Py, when the MWCNT dosage increased from 0.02 g to 0.08 g. This increase can be related to a greater surface area or more

adsorption sites in the high dosage of the adsorbents. In other words, the active sites on the MWCNT surface, can be improve the transfer of phenol species to the adsorbent surface. In addition, the highest phenol sorption is obtained by MWCNT-Py which could be attributed to the interaction of phenol with the functional groups of the presence in MWCNT-Py, such as COOH, C=O, C=S, C=N and NH groups, as compared to MWCNT-COOH (Figure 5b).

a)

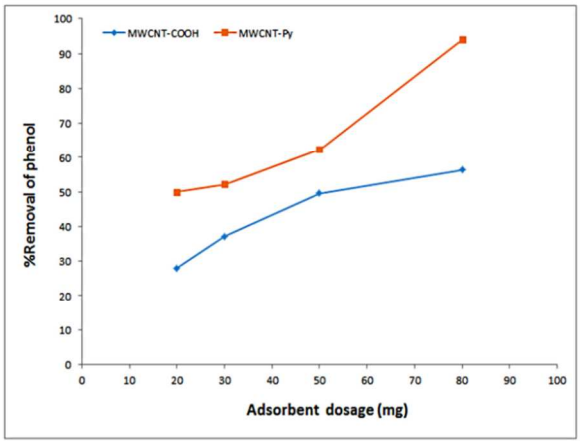

b)

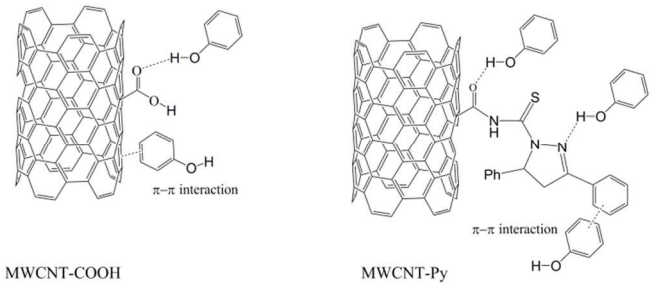

Fig 5. (a) Effect of MWCNTs dosage on the adsorption of phenol from aqueous solution (experimental conditions: pH 7; ultrasonic time, 30 min; phenol concentration, 100 mg/L). (b) A diagram of the mechanism for adsorption of phenol by MWCNTs. In MWCNT-Py, there are three possibilities for phenol sorption in comparing to one for MWCNT-COOH.

3.2.3. Effect of pH

Effect of pH on the uptake of phenol is shown in Figure 6. The adsorbed amount of phenol after equilibrium were calculated at C_0 = 50 mg/l in the pH value range of 3-10 for the comparison purpose. When pH is lower than 7, it has seen a slight increase for MWCNT-COOH and a significant decrease for MWCNT-Py in the removal of phenol. For pH curve of MWCNT-COOH, which fluctuates very little, it can be related to dispersion effect between the aromatic ring and the π electrons of the graphitic structure or electron donor-acceptor interactions between the aromatic ring and the basic surface oxygen, such as carbonyl groups provided that the phenol is in the non-ionized form and the surface groups are either neutral or positively charged.[41,42] In addition, the solubility of phenol is dependent on pH due to weak acidity of phenol in nature, the solubility of phenol decreases with the decrease of pH value (increase of H^+).[14] Thus, in these conditions the removal of phenol by MWCNTs-COOH increased with the decrease of pH value. In other word, there is the inverse relationship between solubility and the phenol adsorption. On the other hand, the MWCNT-Py surface, at low pH values is covered by H^+ ions which hinder phenol molecules from approaching the binding sites on the MWCNTs. Also, amino groups on MWCNT-Py trend to the protonation at 6 > pH which it cause the weak sorption of phenol. At pH > 7, the ionization of the surface carboxylic (for MWCNT-COOH) and phenolic groups occur which result in formation of carboxylate and phenolate anions. In this state, the surface functional groups of MWCNTs, in particular MWCNT-COOH, are either neutral or negatively charged. Hence, the electrostatic repulsion between the identical charges decreases the percentage of adsorption for two adsorbents, in particular MWCNT-Py. In addition, the phenolate anions are solvated by water molecules in the aqueous solutions (more soluble in the aqueous solutions), thus, before adsorption process can carry out, it should be broken stronger adsorbate-water bonds. Therefore, the adsorption of phenol decreases in range of pH > 7. By comparing the sorption percentage of each adsorbent, it was found out that the effect of pH on phenol sorption with MWCNT-Py is more than the MWCNT-COOH. Also, as can be seen in Figure 6, the best sorption percentage for MWCNT-Py at pH=7 was obtained. So, in these experiments to achieve the appropriate condition of adsorption, the pH was adjusted at 6.5-7.

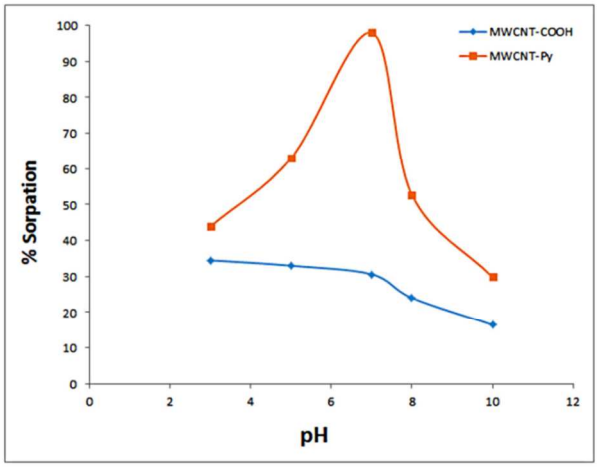

Fig 6. Effect of initial pH on phenol sorption onto MWCNTs. Temperature 298, K.

3.3. Sorption Kinetics

The adsorption parameters derived from the application of the pseudo-first-order equation (K_1 and q_e), the pseudo-second-order equation (K_2, q_e), Elovich's equation (a and b) and intra-particle diffusion (K_{id}) were calculated and listed in Table 2. In addition, linear plots of the kinetic models were presented in Supplementary data. The low correlation coefficients, R^2, of the pseudo-first-order and Elovich models for MWCNT-COOH suggest that both models are inapplicable to fit the kinetic experimental data. The correlation coefficient of the pseudo-second-order model is 0.9900 which agree well with the experimental data. This indicates that the kinetic modeling of phenol adsorbed by the MWCNT-COOH belongs to the pseudo-second-order kinetic model. As can be seen from Table 2, for

Table 2. Parameters of pseudo-first-order, pseudo-second-order, Elovich and intra-particle diffusion models for phenol sorption onto MWCNTs. Temperature, 298 K; initial phenol concentration, 50 mg L^{-1}; mass of MWCNTs, 30 mg; volume of solution, 15 mL; and pH of the sample solution, 7.0.

	Pseudo-first-order model			Pseudo-second-order model			Elovich model			Intra-particle diffusion model	
	k_1(min^{-1})	q_e(mg/g)	R^2	K_2(g $mg^{-1}min^{-1}$)	q_e(mg/g)	R^2	*a*	*b*	R^2	K_{id}(mg g^{-1} $min^{-0.5}$)	R^2
MWCNT-COOH	0.0958	6.811	0.9863	0.0101	10.00	0.9900	1.95	0.427	0.966	1.466	0.9754
MWCNT-Py	0.144	39.3	0.9922	0.00113	43.67	0.9494	4.51	0.1004	0.9855	6.895	0.9472

MWCNT-Py it was observed that the R^2 value of pseudo-first-order kinetic model (0.9922) is significantly higher than that of pseudo-second-order model (0.9494). In addition, the Elovich model was also relatively successful in describing the kinetics of adsorption by the MWCNT-Py. However, the pseudo-first-order model fit better and more precise than the Elovich model. Therefore, the pseudo-first-order model is certainly the most recommendable model for description of the adsorption of phenol on MWCNT-Py and could be used to determine the equilibrium sorption capacity, rate constants, and removal percentage of phenol.

The intra-particle kinetic model of phenol sorption for two adsorbents is shown in Figure 7. The nonzero intercepts of the plots in each case were a clear indication that intra-particle diffusion is not the rate-limiting step of the sorption mechanism. In other words, the intra-particle diffusion model is not the only rate-controlling step. The difference in the rate of mass transfer during the initial and final stages of adsorption can be cause the deviation of the straight lines from the origin. According to Figure 7, it is clear that intra-particle diffusion of phenol within adsorbents occurred in two stages as the plots contain two different straight lines. The initial adsorption stage is rapid for both MWCNTs, in particular MWCNT-Py, so that it involve from 0 to 15 min for MWCNT-COOH and 0 to 20 min for MWCNT-Py, which is due to the fast diffusion of the phenol from the aqueous phase to the outer-surface of MWCNTs. The second stage is a slow adsorption and is from 15 to 30 min for MWCNT-COOH and from 20 to 30 min for MWCNT-Py which could be attributed to the intra-particle diffusion of the phenol molecules into the porous structure of the adsorbents. Therefore, these results confirm which both the external surface sorption and intra-particle diffusion participate in the process of the phenol adsorption by MWCNTs.

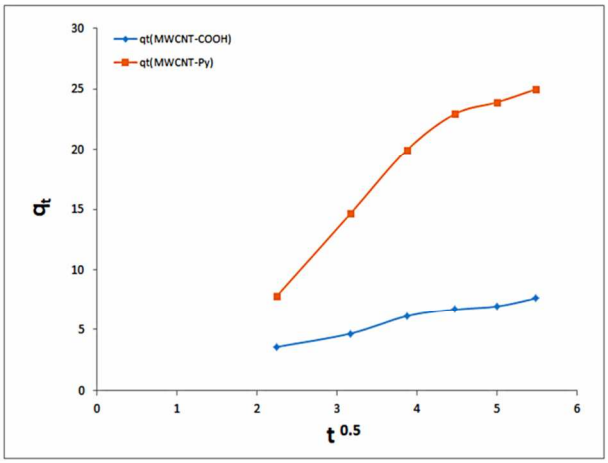

Fig 7. Linearized intra-particle diffusion kinetic model of phenol sorption onto MWCNTs.

3.4. Adsorption isotherms

In general, adsorption isotherms are the mathematical equations describing the ratio between the adsorbed amounts and the remaining in the solution of a material at a constant temperature and pH. In other word, it indicates how a substance from the aqueous media transfers to a solid-phase when the adsorption process reaches an equilibrium state. In this study, six equilibrium isotherm models, Langmuir, Freundlich, Tempkin, Halsey, Harkins-Jura and Fowler-Guggenheim along with certain constant values, which express the surface properties and affinity of the adsorbent, have been used to describe the equilibrium nature of adsorption. All plots of adsorption isotherms are presented in Supplementary data.

3.4.1. Langmuir isotherm

The Langmuir model [43,44] assumes which monolayer adsorption of the molecules can only occur at definite localized sites with the uniform energies of adsorption onto the surface without transmigration of the adsorbate in the plane of the surface. In addition, this empirical model refers to homogeneous adsorption and that there is not any lateral interaction and steric hindrance between the adsorbed molecules. The Langmuir equation for homogenous surface can be written as follows:

$$q_e = \frac{b\, q_m C_e}{1 + bC_e}$$

where q_e (mg g^{-1}) and C_e (mg L^{-1}) are the amount of solute adsorbed per unit weight of adsorbent at equilibrium and phenol concentration at equilibrium, respectively. q_m (mg g^{-1}) is the maximum adsorption capacity, and b is the adsorption equilibrium constant (L mg^{-1}) that is related to the free energy of adsorption. The Langmuir isotherm parameters can be obtained from four different linear forms as shown in Table 3. Among four models, the values of the obtained regression coefficients from Type-2 equation for both adsorbents indicate which the adsorption of phenol on the MWCNTs follows the Langmuir isotherm. In other words, the best equation for the interpretation of experimental data is that of Type-2, which is

Table 3. Langmuir isotherm parameters for phenol removal by MWCNTs.

Adsorbents	Langmuir models	The calculated parameters			
		q_m(mg/g)	b(L/mg)	R^2	Plot
	Type 1	Ultrasound method			
MWCNT-COOH	$\frac{C_e}{q_e} = \frac{1}{bq_m} + \frac{C_e}{q_m}$	21.55	0.0132	0.9945	$\frac{C_e}{q_e}$ vs. C_e
MWCNT-Py		39.22	0.0232	0.9698	
		Stirring method			
MWCNT-COOH		26.45	0.00398	0.9932	
MWCNT-Py		36.90	0.00888	0.9397	
	Type 2	Ultrasound method			
MWCNT-COOH	$\frac{1}{q_e} = \frac{1}{q_m} + \frac{1}{bq_mC_e}$	19.53	0.0152	0.9995	$\frac{1}{q_e}$ vs. $\frac{1}{C_e}$
MWCNT-Py		31.35	0.0326	0.9975	
		Stirring method			
MWCNT-COOH		26.25	0.00402	1.0000	
MWCNT-Py		32.23	0.0105	0.9982	
	Type 3	Ultrasound method			
MWCNT-COOH	$q_e = q_m - \frac{q_e}{bC_e}$	20.904	0.0138	0.9848	q_e vs. $\frac{q_e}{C_e}$
MWCNT-Py		35.407	0.0274	0.9218	
		Stirring method			
MWCNT-COOH		26.593	0.00396	0.9909	
MWCNT-Py		33.847	0.00997	0.8889	
	Type 4	Ultrasound method			
MWCNT-COOH	$\frac{q_e}{C_e} = bq_m - bq_e$	21.176	0.0136	0.9848	$\frac{q_e}{C_e}$ vs. q_e
MWCNT-Py		37.38	0.0252	0.9218	
		Stirring method			
MWCNT-COOH		26.95	0.0039	0.9909	
MWCNT-Py		36.85	0.0089	0.8889	

presented the highest coefficient of correlation for both MWCNTs as compared to other equations. In addition, Langmuir constants for the uptake of phenol in the absence of ultrasound (stirring method) are summarized in Tables 3 for comparison purpose. According to Table 3, the value of q_m for MWCNT-Py was greater than for MWCNT-COOH in the presence and absence of ultrasound**.** This indicates that the functional groups on the surface of MWCNT-Py have relatively stronger affinity for phenol adsorption. On the other hands, the values of Langmuir parameters (b, q_m) are obtained from the four linear expressions, which they were difference. It can be related to the change of the error structure of standard least-squares method when the transformations of non-linear model to linear forms are performed. The essential characteristics of Langmuir isotherm can be expressed in terms of dimensionless equilibrium parameter or separation factor, R_L, as follows: [9, 36]

$$\boldsymbol{R_L = \frac{1}{1 + bC_0}}$$

where b is the Langmuir constant and C_0 is the initial concentration of adsorbate in solution. The values of R_L indicate the type of isotherm to be irreversible ($R_L = 0$), favorable ($0 < R_L < 1$), linear ($R_L = 1$) or unfavorable ($R_L > 1$). The values of R_L in this work we found to be at around 0.397-0.868 for MWCNT-COOH and 0.235-0.754 for MWCNT-Py, indicating a favorable behavior toward phenol adsorption.

3.4.2. Freundlich isotherm

Freundlich isotherm [44,45] can be applied to multilayer adsorption and the heterogeneous surfaces with non-uniform distribution of adsorption heat. This empirical model is:

$$\boldsymbol{q_e = K_F C_e^{1/n}}$$

where K_F is an empirical constant related to the sorption capacity of the adsorbent (L mg^{-1})(L $g^{-1})^{1/n}$ and constant n is a constant indicative of the intensity of the adsorption and varies with surface heterogeneity and affinity. The linearized form of the Freundlich equation is:

$$\boldsymbol{\ln q_e = \ln K_f + \frac{1}{n} \ln C_e}$$

By fitting the experimental data to the Freundlich equation, the value of k_f and n can be calculated by plotting ln q_e versus ln C_e and the results are represented in Table 4. It is known which n values gives an indication on the favorability of adsorption. On the basis, n values between 1 and 10 and less than 1 represent favorable and poor, respectively, sorption process. The high correlation coefficients of MWCNT-COOH (0.9956) and MWCNT-Py (0.9962) show which Freundlich model befits for the interpretation of experimental data. In addition, the values of n for MWCNT-COOH and MWCNT-Py

Table 4. The parameters of the different isotherm models for phenol removal by MWCNTs (Contact time, 30 min; Stirring speed, 300 rpm). The stirring method has been added for comparison purpose.

Adsorbents	Isotherm models	The calculated parameters			Plot
	Freundlich	**K_f (mg/g)(mg/L)^n**	**n**	**R^2**	
		Ultrasound method			
MWCNT-COOH	$\ln q_e = \ln K_f + \frac{1}{n}\ln C_e$	0.451	1.34	0.9956	$\ln q_e$ vs. $\ln C_e$
MWCNT-Py		1.358	1.40	0.9962	
		Stirring method			
MWCNT-COOH		0.1315	1.12	0.9986	
MWCNT-Py		0.4491	1.214	0.9945	
	Temkin	**K_1(L/g)**	**K_2**	**R^2**	
		Ultrasound method			
MWCNT-COOH	$q_e = K_1 \ln K_2 + K_1 \ln C_e$	3.668	0.210	0.9613	q_e vs. $\ln C_e$
MWCNT-Py		6.843	0.367	0.9443	
		Stirring method			
MWCNT-COOH		2.4411	0.139	0.9325	
MWCNT-Py		4.9283	0.198	0.9420	
	Halsey	**K_H**	**n_H**	**R^2**	
		Ultrasound method			
MWCNT-COOH	$\ln q_e = \frac{1}{n_H}\ln K_H - \frac{1}{n_H}\ln\frac{1}{C_e}$	0.344	1.337	0.9954	$\ln q_e$ vs.$\ln 1/C_e$
MWCNT-Py		1.531	1.401	0.9962	
		Stirring method			
MWCNT-COOH		0.1029	1.121	0.9986	
MWCNT-Py		0.378	1.214	0.9944	
	Harkins-Jura	**A_{HJ}**	**B_{HJ}**	**R^2**	
		Ultrasound method			
MWCNT-COOH	$\frac{1}{q_e^2} = \frac{B_{HJ}}{A_{HJ}} - \frac{1}{A_{HJ}}\log C_e$	3.389	1.740	0.8360	$1/q_e^2$ vs.log C_e
MWCNT-Py		12.64	1.564	0.8332	
		Stirring method			
MWCNT-COOH		0.739	1.7812	0.828	
MWCNT-Py		4.073	1.692	0.8340	
	Fowler-Guggenheim	**W (KJ/mol)**	**K_{FG}**	**R^2**	
		Ultrasound method			
MWCNT-COOH	$\ln\frac{C_e(1-\theta)}{\theta} = -\ln K_{FG} + \frac{2W\theta}{RT}$	-29.6987	0.00001598	0.988	$\ln C_e(1-\theta)/\theta$ vs. θ
MWCNT-Py		-22.1594	0.000004.08	0.9839	
		Stirring method			
MWCNT-COOH		-91.982	6.24×10^{-8}	0.9461	
MWCNT-Py		-33.890	1.92×10^{-6}	0.9290	

were found 1.34 and 1.40, respectively, indicating that the sorption of phenol molecules is favorable at the described experimental conditions. This implies that the Freundlich model could represent the data reasonably well for both adsorbents. This isotherm describes reversible adsorption and is not restricted to the formation of monolayer. This means that the assumption of multilayer adsorption is in agreement with the experiment in the studied concentration range.

3.4.3. Tempkin isotherm

Tempkin [46] suggested that heat of adsorption of all molecules in the layer would decrease linearly rather than logarithmic with the surface coverage due to the existence of adsorbent-adsorbate interactions. In addition, it assumes that the adsorption is characterized by a uniform distribution of the binding energies, up to some maximum binding energy. The linearized form of Temkin model is given by:

$$q_e = K_1 \ln K_2 + K_1 \ln C_e$$

where k_1 is related to the heat of adsorption (L/g) and K_2 is the dimensionless Tempkin isotherm constant. Tempkin parameters (k_1 and k_2) can be determined from the linear plots of q_e and ln C_e. The values of Tempkin constant together with the regression coefficients are presented in Table 4 for the adsorption of phenol on MWCNT-COOH and MWCNT-Py. The low regression coefficients of MWCNTs-COOH and MWCNTs-Py show which this model could not interpret the data reasonably for both adsorbents.

3.4.4. Halsey isotherm

Halsey isotherm model [47,48] can be used to the multilayer adsorption systems. If the experimental data to this equation well is fitted, it indicates the heteroporous nature of the MWCNTs. This equation can be given as:

$$\ln q_e = \frac{1}{n_H}\ln K_H - \frac{1}{n_H}\ln\frac{1}{C_e}$$

where K_H and n_H are the Halsey constants, which can be obtained from the slope and the intercept of the linear plot based on ln(q_e) versus ln 1/C_e, respectively. The related Halsey isotherm parameters are calculated and tabulated in Table 4. As can be seen in Table 4, the values of regression coefficients for both MWCNTs are more than 0.99, which show very well agreement to the phenol adsorption on samples. This finding implies that phenol adsorption on adsorbents obeys the Halsey isotherm model and also, confirm the nature of their multilayer adsorption.

3.4.5. Harkins-Jura isotherm

Harkin-Jura adsorption [49] isotherm can be used to the multi-layer adsorptions and that it assumes the existence of the heterogeneous pore distribution in the surface of adsorbents. This model can be expressed as:

$$\frac{1}{q_e^2} = \frac{B_{HJ}}{A_{HJ}} - \frac{1}{A_{HJ}}\log C_e$$

The Harkins-Jura isotherm parameters, B_{HJ} and A_{HJ} (the Harkins-Jura constants), can be obtained from the linear plot of $1/q_e^2$ against log C_e. It can be seen in Table 4 that the values of R^2 are obtained less than 0.99 for both adsorbents, which indicate the inapplicability of this model for the phenol adsorption on MWCNTs.

3.4.6. Fowler-Guggenheim isotherm

Fowler-Guggenheim model[50] explains whether the lateral interaction of the adsorbed molecules into MWCNTs has been existed or not. The linearized form of this model is expressed by:

$$\ln\frac{C_e(1-\theta)}{\theta} = -\ln K_{FG} + \frac{2W\theta}{RT}$$

where K_{FG} is the Fowler-Guggenheim equilibrium constant (L mg^{-1}), θ = (1-Ce/Co) is the degree of surface coverage, W is the interaction energy between adsorbed molecules (kJ mol^{-1}), R is the universal gas constant and equal to 8.314 J mol^{-1} K^{-1} and T is the absolute temperature (K). The W values in the equation determine the interactions between the adsorbed molecules. Therefore, if W is positive, the heat of adsorption due to the increased interaction between adsorbed molecules will increase with loading of adsorbate. In other words, the interaction between the adsorbed molecules is attractive. Conversely, if W is negative, the interaction among adsorbed molecules is repulsive and hence, the heat of adsorption decrease with loading. When there is no interaction between adsorbed molecules, it is W= 0. The values of K_{FG} and W were evaluated from the intercept and the slope, respectively, of the linear plot of ln C_e(1-θ)/θ versus θ based on experimental data. The adsorption data for the phenol adsorption onto both adsorbents were calculated and summarized in Table 4. According to Table 4, it is observed which the linearization is relatively good and the interaction energy, W, is negative, which indicates the presence of repulsion between the adsorbed molecules by both MWCNTs.

4. Conclusions

We have firstly introduced pyrazoline derivative groups on the surface of CNTs to form MWCNT-Py which was characterized by FT-IR, TEM and TGA. The study shows that MWCNT-Py has ideal performance for adsorption of phenol. The results showed that MWCNT-Py has higher sorption capacity respect to MWCNT-COOH in ultrasound condition. The adsorption isotherms of phenol have been well fitted by Langmuir, Freundlich and Halsey models which mean physical adsorption occurred and that it were expected the mixed isotherm models for the adsorption of phenol under ultrasonic conditions. In addition, W values for both MWCNTs were negative, which show the presence of the repulsive among adsorbed molecules. The sorption kinetics was found to follow pseudo-first-order model for MWCNT-Py.

Acknowledgements

The financial and encouragement support provided by Research vice Presidency of Ayatollah Amoli branch, Islamic Azad University.

Notes and references

Department of Chemistry, Ayatollah Amoli Branch, Islamic Azad University, Amol, Iran. E-mail: h.tahermansuri@iauamol.ac.ir

Electronic Supplementary Information (ESI) available: [All plots of adsorption kinetics and isotherms are presented in Supplementary data].

1 E. Sabio, M.L.G. Martin, A. Ramiro, J.F. Gonzalez, J.M. Bruque, L.L. Broncano, J.M.J. Encinar, *J Colloid Interface Sci*, 2001, **242**, 31.
2 J. Huang, X. Wang, Q. Jin, Y. Liu, Y. Wang, *J. Environ.Manage*, 2007, **84**, 229.
3 O. Hamdaoui, E. Naffrechoux, J. Sptil, C. Fachinger, *Chem. Eng. J,* 2005, **106**, 153.
4 F.A. Banat, V. Al-Bashir, S. Al-Asheh, O. Hayajneh, *Environ. Pollut,* 2000, **107**, 391.
5 A. Knop, L.A. Pilato, *Phenolic Resins-Chemistry: Applications and Performance*, Springer-Verlag,1985.
6 X. Ren, C. Chen, M. Nagatsu, X. Wang, *Chem. Eng. J,* 2011, **170**, 395.
7 A. Aqel, K.M.M. Abou El-Nour, R.A.A. Ammar, A. Al-Warthan, *Arabian J. Chem*, 2012, **5**, 1.
8 D. Shao, Z. Jiang, X. Wang, J. Li, Y. Meng, *J. Phys. Chem. B,* 2009, **113**, 860.
9 H. Tahermansouri, M. Beheshti, *Bull. Korean Chem. Soc,* 2013, **34**, 3391.
10 K. Yang, W.H. Wu, Q.F. Jing, L.Z. Zhu, *Environ. Sci. Technol*, 2008, **42**, 7931.
11 G.D. Sheng, D.D. Shao, X.M. Ren, X.Q. Wang, J.X. Li, Y.X. Chen, X.K. Wang, *J. Hazard. Mater*, 2010, **178**, 505.
12 Q. Liao, J. Sun, L. Gao, *Carbon*, 2008, **46**, 553.
13 M.A. Salam, R.C. Burk, *Appl. Surf. Sci*, 2008, **255**, 1975.
14 R. Arasteh, M. Masoumi, A. M. Rashidi, L. Moradi, V. Samimi, S. T. Mostafavi, *Appl. Surf. Sci,* 2010, **256**, 4447.
15 O. Hamdaouia, E. Naffrechoux, *J. Hazard. Mater*, 2007, **147**, 381.
16 P. Podkoscielny, K. Nieszporek, *J Colloid Interface Sci*, 2011, **354**, 282.

17 O. Hamdaoui , E. Naffrechoux, *Ultrason. Sonochem*, 2009, **16**, 15.
18 R.-S. Juang, S.-H. Lin, C.-H. Cheng, *Ultrason. Sonochem*. 2006, **13**, 251.
19 O. Hamdaoui, E. Naffrechoux, L. Tifouti, C. Pétrier, *Ultrason. Sono chem*, 2003, **10**, 109.
20 M. Breitbach, D. Bathen, *Ultrason. Sonochem*, 2001, **8**, 277.
21 S. A. Kosa, G. Al-Zhrania, M. A. Salam, *Chem Eng J*, 2012, **181-182** ,159.
22 J. Hu, DD. Shao, CL. Chen, GD. Sheng, XM. Ren, XK. Wang, *J Hazard Mater*, 2011, **185**, 463.
23 M. Hadavifar, N. Bahramifar, H. Younesi, Q. Li, *Chem Eng J*, 2014 **237**, 217.
24 X. Tian, W. Wang, Y. Wang, S. Komarneni, C. Yang, *Microporous and Mesoporous Materials*, 2015, **207**, 46.
25 Z.Zhang, X.Xu, *Chem Engi J*, 2014, **256**, 85.
26 MA. Salam, MA. Gabal, AY. Obaid, *Synth Met*, 2012, **161**, 2651.
27 WH. Wu, W. Jiang, WX. Xia, K. Yang, BS. Xing, *J Colloid Interface Sci*, 2012, **374**, 226.
28 G. Mamba, XY. Mbianda, PP. Govender, *Carbohyd Polym*, 2013, **98**, 470.
29 Ihsanullah, H. A. Asmaly, T. A. Saleh, T. Laoui, V. K. Gupta, M. A. Atieh, *J Molecular Liquids*, 2015, **206**, 176.
30 LP. Lukhele, RWM. Krause, ZP. Nhlabatsi, BB. Mamba, MNB. Momba, *Desalin Water Treat,* 2011, **27**, 299.
31 DD. Shao, J. Hu, ZQ. Jiang, XK. Wang, *Chemosphere*, 2011, **82**,751.
32 G.D. Vukovic, A. D. Marinkovic, M. Colic, M. D. Ristic, R. Aleksic, A. A. Peric-Grujic, P. S. Uskokovic, *Chem Eng J,* 2010, **157** , 238.
33 Y. Wang, Z. Gu, J. Yang, J. Liao, Y. Yang, N. Liu, J. Tang, *Applied Surface Science*, 2014, **320**, 10.
34 G. Turan-Zitouni, P. Chevallet, F. S. Kiliç, K. Erol, *Eur. J. Med . Chem,* 2000*,* **35**, 635.
35 S. Lagergren, *Handlingar*.1898, **24**, 1.
36 H. Tahermansouri, R. Mohamadian Ahi, F. Kiani, *J. Chin.Chem.Soc*, 2014, **61**, 1188.
37 W. Rudzinski, T. Panczyk, *Langmuir*, 2002, **18**, 439.
38 S.H. Shien, W.R. Clayton, *Soil Sci. Soc. Am. J.* 1980, **44**, 265.
39 W. J. Weber, J. C. Morris, *J. Sanitary Eng. Div*, 1963, **89**, 31.
40 H. Tahermansouri, A. Mirosanloo, *Fullerenes, Nanotubes Carbon Nanostruct*, 2015, **23**, 500.
41 K. Laszlo, P. Podkoscielny, A. Dabrowski, *Langmuir*, 2003,**19**, 5287.
42 Q. Liao, J. Sun, L. Gao, *Colloids Surf A*, 2008, **312**,160.
43 I. Langmuir, *J. Am. Chem. Soc*, 1916, **38**, 2221.
44 K.Y. Foo, B.H. Hameed, *Chem. Eng. J*, 2010, **156**, 2.
45 H.M.F. Freundlich, *J. Phys. Chem*, 1906, **57**, 385.
46 M. J. Tempkin, V. Pyzhev, *Acta Physiol.Chem.URSS,* 1940, **12,** 327.
47 G.D. Halsey, *Adv. Catal*, 1952, **4**, 259.
48 J. Liu, X.Wang, *Sci World J*, 2013, **2013**, Article ID 897159.
49 A. Kausar, H. N. Bhatti, G. MacKinnon, *Colloids Surf. B*, 2013, **111**, 124.
50 R.H. Fowler, E.A. Guggenheim, *Statistical Thermodynamics*, Cambridge University Press, London, 1939, pp. 431-450.